# DETAILED CFX-5 STUDY OF THE COOLANT MIXING WITHIN THE REACTOR PRESSURE VESSEL OF A VVER-1000 REACTOR DURING A NON-SYMMETRICAL HEAT-UP TEST

**Michael Böttcher**

Forschungszentrum Karlsruhe, Institut für Reaktorsicherheit, Hermann-vom-Helmholtz-Platz-1, D-76344 Eggenstein-Leopoldshafen

boettcher@irs.fzk.de

## Abstract

As part of the reactor dynamics activities of FZK/IRS, the qualification of a detailed 3D CFD model of a reactor pressure vessel is a key step in safety evaluations for improving predictive capabilities and acceptability of commercial CFD tools in reactor physics. The VVER-1000 Coolant Transient Benchmark, initiated by OECD, represents an excellent opportunity for validation. In this work a CFD model for the complete VVER-1000 reactor pressure vessel is presented. Due to computational limits simplifications of the core and of some other geometrical details are introduced. The simulated scenario is the heat-up of a single primary coolant loop in case of the isolation of one turbine (loop-1) while the reactor is operating at a low power level. Two transient runs with a first and second order approximation of the spatial discretization are performed. Unexpectedly the first order method reveals better agreement with measured data.

## Key Words

Coolant mixing, CFD-Simulations, CFX-5, VVER-1000, reactor pressure vessel, OECD benchmark

## Introduction

It is an essential aim of CFD investigations to simulate 3D flow phenomena in high complex technical systems. In case of nuclear reactor pressure vessels the scales of interest are spread over several orders of magnitude. The height of an RPV is around 10m and more with an inner diameter of some meters. The smallest geometrical details which have significant influence on mixing phenomena are in a range of 1mm. To resolve this technical system in all details would require a grid far beyond computational capabilities. Therefore, several aspects that have to be considered for developing of a large CFD model such as the available memory of the computational platform for grid development and of the workstation for performing the simulations. For this analyis, we used a 4 node LINUX cluster with 16 GB RAM. Tests with CFX 5.7.1 have shown that this is sufficient for the treatment of single phase flows with standard k-ε turbulence model using a grid of 20 million unstructured cells. For grid generation the tool GRIDGEN is used on Windows XP with 2 GB memory that allows the treatment of 10 million cells. Nevertheless, the response time for a single grid manipulation action for such a case often reaches one hour. CFX-5 allows the treatment of computational domains whose boundary nodes don´t need to match exactly. Those nodes are matched by an interpolative method. For testing and handling such an approach is advisable and in the present case even necessary because the complete grid cannot be handled as one part due to limitations of the grid generation processing. Some other computational limits are given by the pre-processing of CFX 5, where the computational domains and the flow physics are defined. The pre-processing under Windows XP enables the treatment of approximately 30 million unstructured cells.

An essential aspect is given by CFD best practice guidelines [1]. Refinement of the grid should be tested to achieve independency of the solutions from grid spacing. The resulting model of VVER-1000 RPV consists of around 14 million cells and requires computational times up to 2 weeks. Especially the upper plenum consisting of 9.6 million cells is very close to one of our computational limits. The model presented here is a compromise between physical flow treatment due to geometrical simplifica-

tions and detail resolution, manageability, computational costs and time consumption of model development.

**Design and geometrical peculiarities of the VVER-1000 reactor**

The VVER-1000 is a four loop pressurized water reactor with hexagonal fuel assembly design and horizontal steam generators. Operating at nominal conditions with a thermal power of 3000 $MW_{th}$ the system pressure amounts 15.6 MPa with a core inlet coolant temperature of app. 560 K. The mean coolant mass flow rate is at 17.6 tons per second. The plant being investigated is the unit 6, located at Kozloduy, Bulgaria. The overall height of the pressure vessel is around 12.5 m and its inner diameter amounts to 3.6 m. The main inlet and outlet nozzles of the reactor vessel (Ø 0.85 m) are located non-uniformly and asymmetrically with respect to the core symmetry axes. The core is of open type and contains 163 hexagonal fuel assemblies; each one consists of 312 fuel pins. The main design details are shown in Fig. 1. The coolant enters the vessel by the inlets (a), flows downwards through the downcomer (b) and enters the lower plenum by passing a perforated elliptical bottom plate (c). It flows through channels formed by the lower parts of the core support columns (d). The upper part of the support columns serve as flow distributor at core entrance. In this part the columns are perforated and hollow. Due to the small scales of the perforations, this part cannot be modelled directly and hence it is considered only by pressure loss coefficients (e). Crossing the core bottom plate (f) the water enters the core. Towards the upper plenum (grey colour) the flow is heated up by the core (red). On its way through the upper plenum the coolant passes through control rod guide tubes (g) and passes radially two perforated walls (h,i), the first one has a conical shape at its lower section (h). Fig. 2 shows the upper plenum in more detail and greater magnification. A detailed view of the lower plenum is given in Fig. 3.

A more detailed description of the components and geometry can be found in OECD benchmark specifications [2].

**Short description of the developed CFX-5 model**

The developed global model is divided into 3 parts, see Fig. 1: the inlets, downcomer and lower plenum (turquoise); the core (red) and the upper plenum with outlets (grey). The turquoise model part was constructed and provided by Bieder [4] as contribution to the above-mentioned OECD Benchmark.

The model part consisting of the inlets, downcomer, and lower plenum is constructed by 2.6 million unstructured tetra cells. In general the application of hexa cells leads to less numerical diffusion but in high complex geometries the generation of hexa grids may become very time-consuming because up to now no automatically generation procedure is available. Crucial points of this sub-model are the diffuser and the consoles (structures for fixing the core barrel against the downcomer) in downcomer, the perforated elliptic core barrel plate and the core support columns, see Fig. 3. As mentioned above it is insufficient to represent the elliptical bottom plate and the upper part of the core support columns in detail. The purpose of the bottom plate is to equalize the flow profile by a large pressure loss. Additional pressure loss coefficients were introduced to address provided design pressure drops measured between the positions P0, P2, P4, P5 and P6, approximately for nominal steady state conditions. For later-on presented transient calculations these additional loss coefficients were maintained. Fig. 3 shows the distribution of the relative pressure in the lower plenum under nominal steady state conditions of 17.6 tons/s coolant mass flux and 540 K inlet temperature. To achieve a nearly axial flow through the elliptical bottom plate pressure loss coefficients of 600 in axial direction and 10000 in radial direction are introduced. For the upper part of the support columns $\lambda$=50 (isotropic) is assumed. The additional pressure loss in streamwise direction x due to $\lambda$ is obtained by

$$-\frac{\partial p_\lambda}{\partial x} = \lambda \frac{\rho}{2} |u| u \quad ,$$

where u is the velocity component in streamwise direction and ρ is the density of the fluid.

The position of the bottom plate is visible by the zone of contour line agglomeration at the lower parts of the support columns. Pressure maxima in the downcomer can be found just above console elements where the flow locally stagnates.

Fig. 4 presents the core model constructed with 800000 hexagonal cells. The heated length of 3550 mm is divided into 35 axial layers. A detailed resolution of the core, following best practice guidelines, would require around 100 million cells. Due to this fact simplifications had to be introduced. As it is not possible to introduce volume porosities in CFX 5.7.1 and previous versions of CFX 5 the cross section flow area in the simplified model should be preserved in order to get the correct mean flow velocities. In the core of VVER-1000 reactor 46% of the cross section area is blocked by fuel pins. Therefore, the pin area part is left empty in each assembly and the free flow section is represented by an annulus channel of hexagonal shape. Between neighboured assemblies mass and energy exchange is possible.

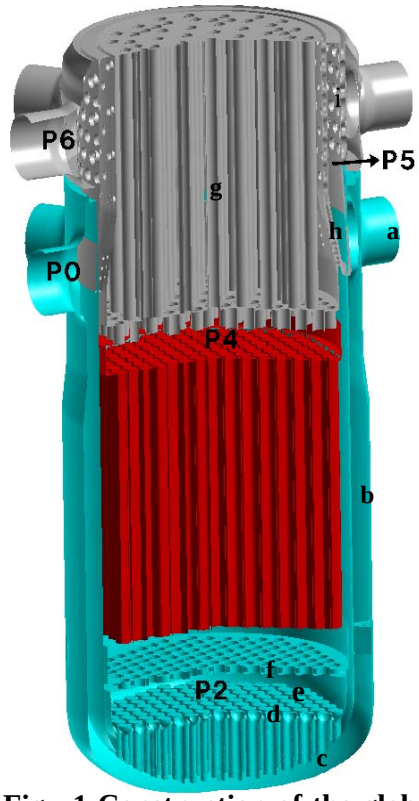


**Fig. 1 Construction of the global model (P: measurement points)**

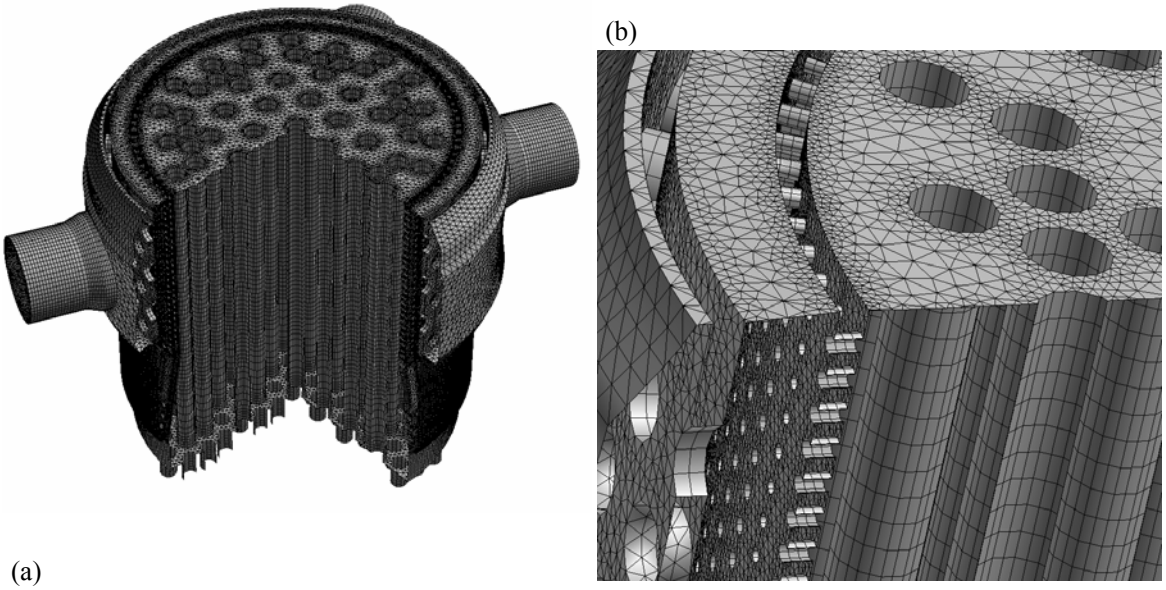


**Figure 2 Grid model of the upper plenum (9.6 millions of cells)**

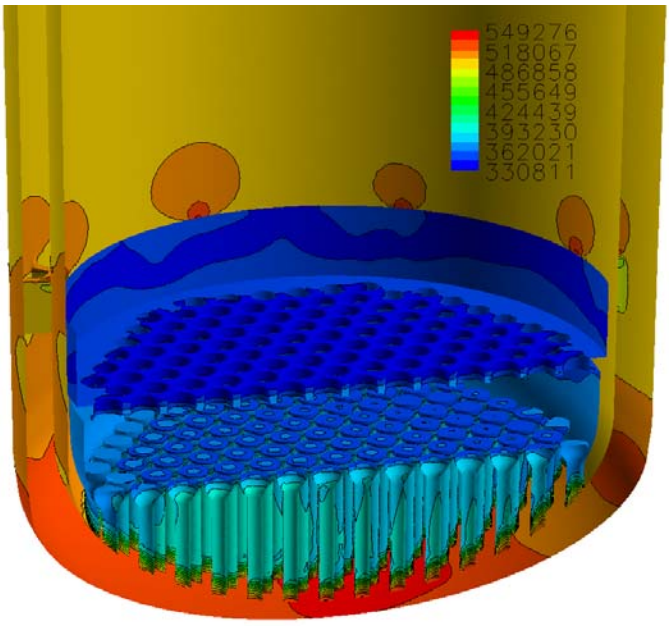


**Fig. 3 The lower plenum coloured with relative pressure [pa]**

In outer positions the assemblies are surrounded by an unheated bypass channel (marked by B in right part of Fig. 4), which carries app. 3% of the total mass flux. Between the bypass channel and neighbouring assemblies heat transport by conduction is possible. The nuclear heat sources, taken from a RELAP5/PARCS simulation [3], are implemented as volumetric heat sources dependent on the assembly position and the axial coordinate. The temperature distribution in the core is shown for a symmetric coolant flux of 17.6 t/s and an inlet temperature of 540 K, see Fig. 4. The core is operating at a low level of 9.4 % of nominal power with a thermal power release of 280 MW. The hotter areas are characteristic for assemblies with higher fuel enrichment.

Because solid pin structures are not modelled the pressure loss would be much lower without introduction of additional pressure loss coefficients. For the assemblies $\lambda=3$ is assumed. For the bypass channel $\lambda=1.2$ is used.

The upper part of the RPV model consists of the core bottom plate, the upper plenum with control rod guide tubes, and the outlets. Essential structures in the upper plenum are control rod guide tubes. The upper plenum is surrounded by a perforated core barrel wall with a conical shape in its lower section containing slot structures and holes. Between the core barrel wall and the outlet nozzles another perforated wall is located. All geometrical structures in this part of the RPV model are geometrically resolved by the grid of 9.6 million cells. Fig. 2 shows details of the mesh in the upper plenum. In order to save cells the grid is locally refined only in regions where strong gradients are expected, as can be seen in Fig. 2b). In radial direction the perforations of the core barrel wall and of the outer wall are modelled by 3 and 2 cells, respectively. This seems to be insufficient to get grid independent solutions of the flow fields. Because memory limit for grid generation was almost reached, further refinement would be only possible by splitting the upper plenum into smaller parts. But this would increase the effort and computational costs again significantly.

The implementation of loss coefficients is a possibility for geometrical model simplification and for adaptation of model pressure distribution with plant data. The various positions where plant pressure data are taken are into account presented in Fig. 1 (P-positions).

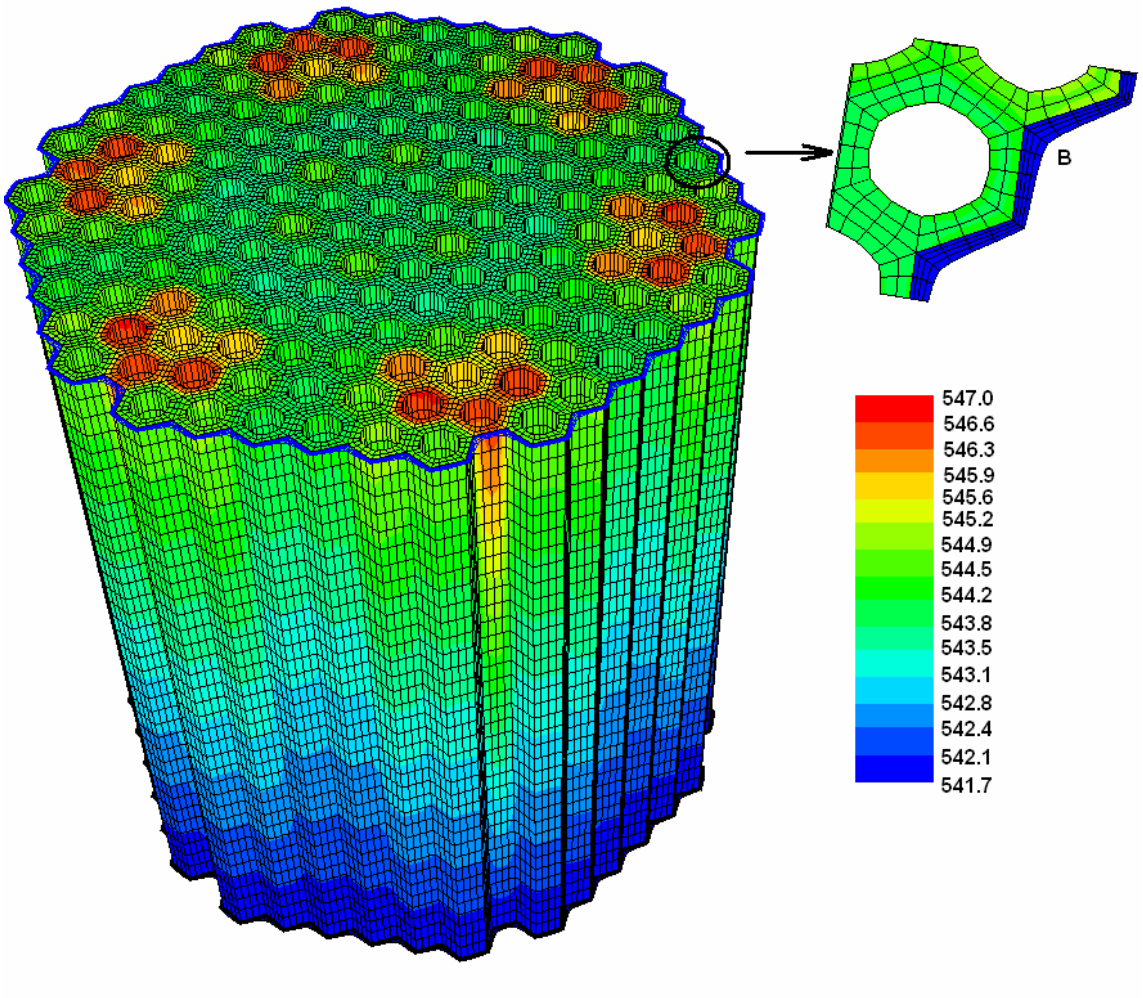


**Fig. 4 The core model with the temperature distribution in [K]**

The locations are at the inlets (P0) and outlets (P6), in the lower plenum below the core support plate (P2), above the core (P4) and at the upper plenum between the perforated walls (P5). The pressure difference P0-P2 was used to evaluate pressure loss coefficients for the elliptical bottom plate and the perforated part of the support columns. As no additional information was available it is assumed that the pressure losses for both component parts are the same. For the core model P4-P2 was used together with the above-mentioned amount of mass flux for the bypass channel to estimate loss coefficients. In the upper plenum model no loss coefficients are required, because all relevant geometrical details are resolved by the fine grid. Tab. 1 presents a comparison between measured pressure data and model data for standard conditions as mentioned before.

| | Δp [Mpa] / measured | Δp [Mpa] / CFX model |
|---|---|---|
| P0-P2 | 0.1971 | 0.202 |
| P2-P4 | 0.1422 | 0.159 |
| P4-P5 | 0.0284 | 0.036 |
| P4-P6 | 0.0363 | 0.041 |
| P0-P6 | 0.376 | 0.402 |

Tab. 1 Comparison of design pressure drops; red coloured model data are upper plenum data obtained without additional pressure loss coefficients

The accuracy of the plant data is ± 0.02 MPa, for the overall pressure loss P0-P6 ± 0.043 MPa are assumed. The pressure differences in the upper plenum are up to 20 % above the plant data. The perforated walls in the upper plenum of VVER-1000 contain two additional holes for the emergency coolant injection. The additional implementation of these bore-holes in the model (Ø 300 mm!) would reduce the pressure differences significantly. But despite of this fact all model data are within the error range of measured data.

The global model is available with following simplifications:

1. No solids are considered. Due to the energy content of steel structures compared with coolant which is some orders of magnitude larger solids are less important. Concerning heat conduction through solids the energy transport by forced convection is much bigger.
2. All outer boundaries are considered adiabatic. The volume-to-surface ratio is large so that heat losses through outer surfaces can be neglected.
3. Several design elements are not resolved by the grid. Their influence is considered only by additional pressure loss coefficients. This simplification is in some parts of significant influence on the mixing processes because the generation of turbulence is not represented properly.
4. In case of scenarios with tight neutronic/thermal hydraulic interactions, a more frequent update of the core heat sources would be necessary.
5. Several components are not implemented or strongly simplified, such as pins and spacers.

**Description of the coolant mixing test to be investigated**

During the plant-commissioning phase of the Kozloduy nuclear power plant special experiments were performed to study the mixing of loop flows in the pressure vessel. Due to the low reactor power the described test can be considered as a pure thermo-hydraulic problem. At around 9,4 % of the nominal power level one of the four steam generators is isolated from steam and feed water so that the temperature in the disturbed loop started to rise. During this process the nuclear power generation was maintained nearly at its initial level of 281 MW (286 MW at the final state), so that a linear time dependency is assumed for simulation.

In about 20 minutes the temperature of the disturbed loop raised by 13.6 K while the other loops are left at around 540 K. The process reaches a stabilized final state after 30 minutes.

As boundary conditions the thermal power of the reactor, the transient flow rates, and temperatures at the inlets are taken from the benchmark specifications as given in Fig. 5 and Fig. 6. While the mass fluxes from loop 3 and 4 nearly remain constant the flux from loop 1 decreases by around 3.5%. This can be understood by the decrease of density due to the increase of temperature. Maintaining the mass flux would require some more pump power due to a higher pressure loss because of an increased mean velocity. So a constant power of the pump leads to a decrease of the mass flux.

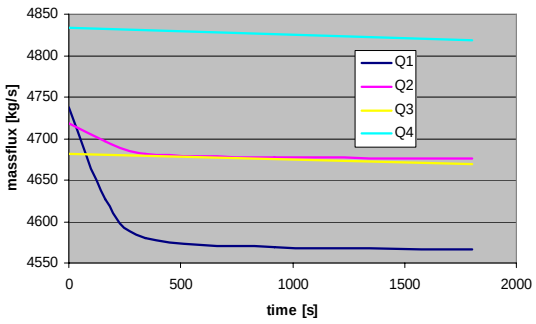


**Fig. 5** Mass fluxes at inlet

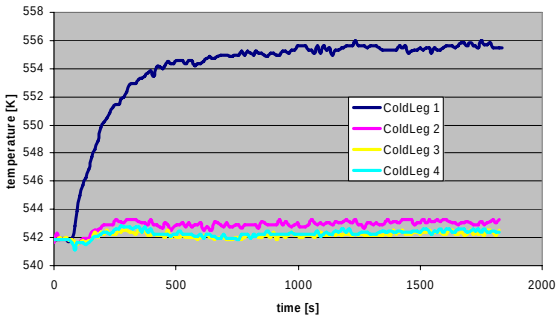


**Fig. 6** Inlet temperatures

The original task of the benchmark was to calculate temperatures and mass fluxes at the assembly inlets. With the extension of our computational model to all parts of the RPV, additional comparisons with temperature measurements at the fuel assembly outlets and with hot leg temperature data are now possible.

Furthermore loop-to-loop mixing coefficients derived from experimental data can be compared with simulations. Loop-to-loop mixing coefficients $K_{ij}$ in the flow path from cold leg i to hot leg j are defined as ratio of the coolant flow from loop i into loop j, to the total flow in loop j. In our model this can be realized by the transport of a passive tracer for which only an additional transport equation has to be solved. The tracer concentration is set to 1 at the inlet of cold leg i. Due to convective transport based on the velocity fields the spatial mass fraction of the tracer is available which is equivalent to a loop mixing coefficient. The experimental mixing coefficients are derived from thermocouple measurements at the core outlet. At low core power temperature can be used as tracer. If one loop is significantly hotter as in the presented scenario then from local temperature measurements under the neglection of diffusion and at known heat-up of the core the origin of the fluid described by $K_{ij}$ can be derived. For each loop a heat-up experiment was performed in order to derive mixing coefficients. In fact numerical and experimental mixing coefficients can only be compared if the thermohydraulic conditions are similar. Details of the method can be found in [5] and [6].

For the modelling of turbulence a standard k-ε model was used. The simulations were performed with a time step of 12 s. Time steps from 6s up to 30 s were tested but only for the first 300s of the scenario. The differences in the results were negligible. At time steps of 12s the local Courant numbers are much higher than 1 because the flow needs at a massflux of 17.6t/s around 4s in order to pass through the vessel. On the other hand the heat-up of loop 1 mainly happens within the first 600s so that the conditions inside the vessel can be considered as quasi steady-state. From this point of view with a time step of 12s together with an implicit time integration method one should be able to resolve the time dependency of this scenario.

The time integration was performed by using a second-order implicit Euler-Backward method. For spatial discretization a first order donor cell method was used. Alternatively the standard high order method from CFX 5 by Barth and Jesperson [7] with 2nd order accuracy was applied.

Both runs were started from a converged steady-state solution using the donor cell method based on the boundary conditions given by Fig. 5 and 6 at t=0s. As convergence criteria the rms residual values mainly for pressure and velocity components and the global balances for momentum and energy equations were checked. For the initial steady state solution the normalized residuals were found in the range of $10^{-4}$ and global balances were fulfilled by $8*10^{-3}$. During the transient for the donor cell method the residuals increased up to $5*\ 10^{-4}$ and $10^{-2}$ for the global balances. For the 2nd order method residuals of $10^{-3}$ and $2*10^{-2}$ for the global balances were achieved. Following the guidelines from CFX the transient run with the 2nd order method is only bad converged and can be used only for technical studies whereas in the other case the convergence is of good quality.

**Discussion of selected results**

At first a comparison with thermocouple measurements at the assembly outlets is presented. Figure 7 shows the results for the runs with 1st and 2nd order method at t=0s and at t=1800s. The numbering of the fuel assemblies and the location of the loops is shown in Figure 8.

Due to design constraints not all assemblies are equipped with sensors. The accuracy of the measurements is given as $\pm$2K. All numerical results lie within the experimental error band. At the low power level of 281-286MW the flow in the core is heated up by 5K locally. The up to 3 times larger heat up of loop 1 is based on the missing heat removal as it is isolated from its heat exchanger. A new steady state is achieved when the nuclear heat released into loop 1 by one circulation of the flow through the core is transported by mixing into the other loops, where it is then removed by the other heat exchangers being in operation. Because the energy exchange between the loops depends on its temperature

differences a continuous heat up of loop 1 together with a moderate increase in the other loops takes place until new steady state temperature distributions are reached.

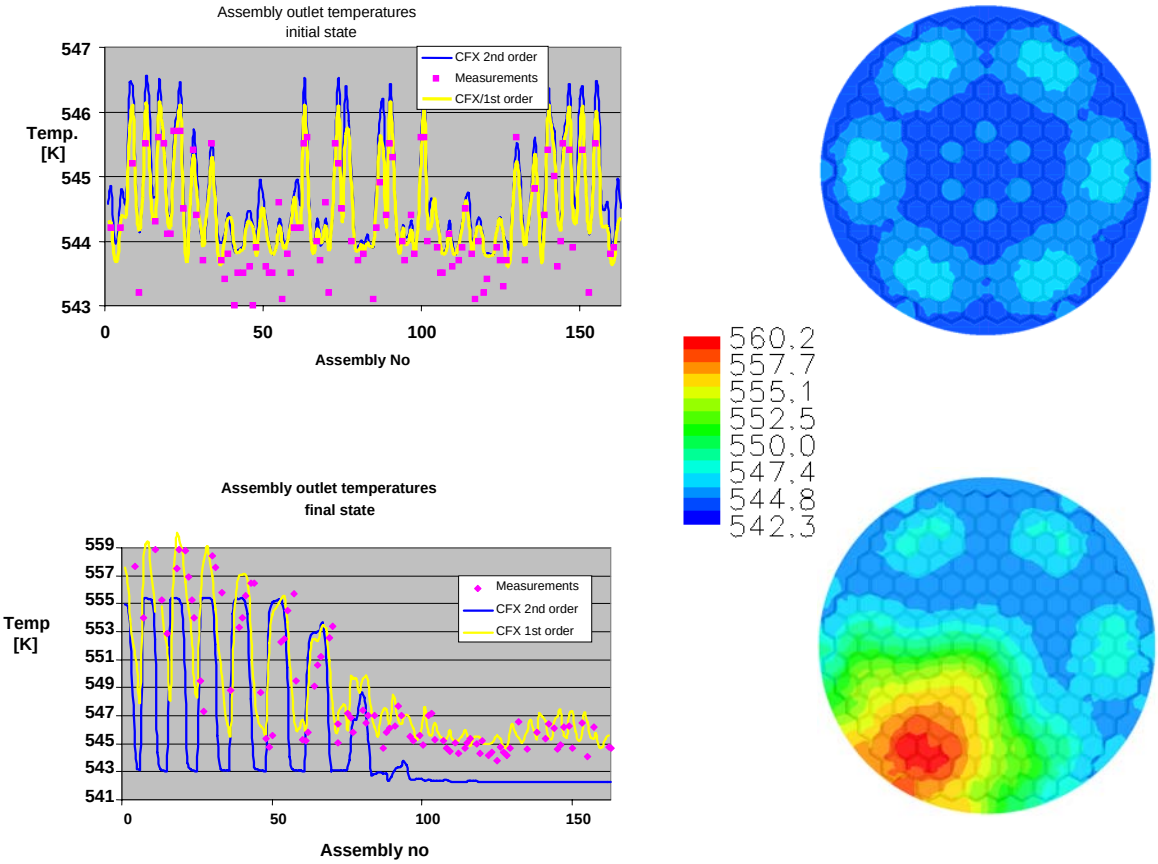


**Figure 7 Assembly outlet temperatures [K] at initial state and final state**

The initial state temperatures seem to be over-predicted by both methods (Fig. 7), but this trend is much smaller than the measurement accuracy. The 2nd order method shows a slightly larger overestimation of local temperature maxima. The final state temperature distribution at the assembly outlets is dominated by the heat up of loop 1 which is nearly 3 times larger than the nuclear heat up.

In the simulations presented here, the fuel assembly inlet and outlet temperatures predicted using the 1st order method are closer to the experimental data than the ones calculated with the 2nd order method.

An explanation for this is given by the following considerations: Some design details like the elliptical bottom plate and perforated part of the support columns are of significant influence on mixing processes but are only taken into account by pressure loss coefficients. So turbulence production of these parts is missing. A 1st order method is numerically more diffusive and acts like an additional source of turbulence. Another point was the observed much better convergence of the 1st order method than that of the 2nd one. The residuals of velocity, pressure and temperature were one order of magnitude smaller than the ones of the calculation with the 2nd order method. Following the code guidelines the convergence quality of the 1st order run was good while the 2nd order run accuracy could be characterized as critical.

The computational time for the steady state analysis was around 4 days for both runs. The simulation of the transient took around 3 days for 1st order and 2 weeks for the 2nd order run on a LINUX-cluster with Xeon 2 GHz processors. All runs were performed with a parallel setup of 4 processes.

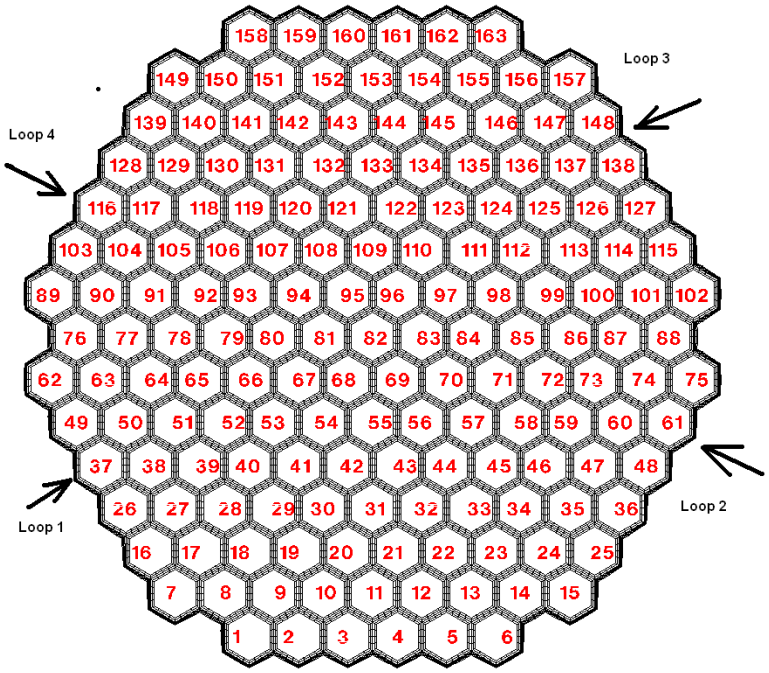


**Fig. 8 Numbering of the fuel assemblies and position of the loops**

The comparison of calculated and those mixing coefficients derived from experimental data show similar trends. Fig. 9 shows mixing coefficients concerning cold leg 3 for plant data and again for 1st order and 2nd order run. The experimental data are derived from temperature measurements taken at the assembly outlets. As mentioned before the numerical data were obtained by transport of a passive tracer whose value was set to 1 at inlet 3. The right part of Fig. 9 shows the global tracer distribution. The spread of the mixing zones in the downcomer is well visible. The distribution presented here is taken from the 1st order case. The 2nd order case shows some overshooting because the tracer values locally reached 1.02 and slightly negative values of -0.01 which refers to convergence problems. The range of values for the 1st order case is between 1.0 and -1.0e-06. The slightly negative values can be explained with numerical inaccuracies. The high order method shows an over-prediction in the mixing zones, especially in the surrounding of the assemblies 90, 100 and 110, see left part of Fig. 9.

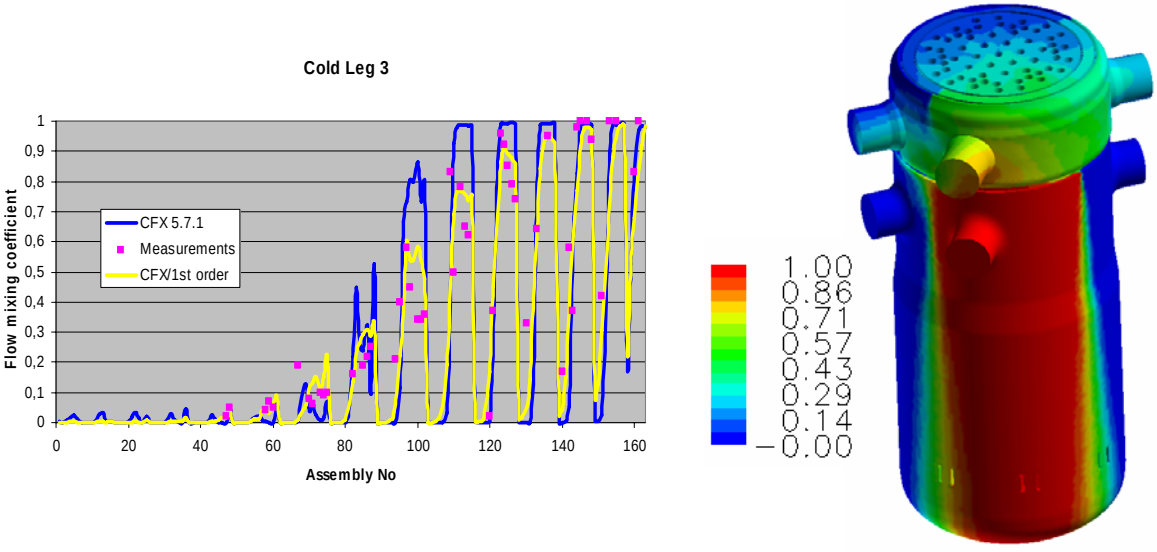


**Fig. 9 Mixing coefficient for the cold leg 3 at the initial steady state conditions**

A comparison of the predicted mixing coefficients with the data for the other loops showed the same tendencies as for the loop 3. Finally a comparison of the calculated coolant outlet temperatures of the four loops with the measurement data are presented, see Fig. 10-13. The temperature development in

loop 1 is dominated by the temperature rise of more than 12 K, see Fig. 10. Both runs show good agreement with plant data but again the 1st order method is closer to the experiments. The other loops also show a temperature rise because they are affected by loop 1 due to mixing effects in the down-comer as demonstrated before. The temperature increase in the other loops is much smaller and only in the range up to 1.5K. The temperature rise at the outlet of loop 2 is over-predicted by CFX-5 with both methods, see Figure 11. The reason therefore is not clear because nearly the same behaviour was found using a smaller timestep of 6s. On the other hand the overprediction is around 1.4 K which is below the error range of the measurements. At loop 3 (Fig. 12) the plant data show some oscillations with slightly decreasing amplitude. Between 0 and 500 s the high-order method reflects the swings of the plant data. After 700s the temperatures are slightly underestimated. The 1st order method predicts the first temperature rise quite well but doesn't show any tendency for smaller oscillations as found in the measurements.

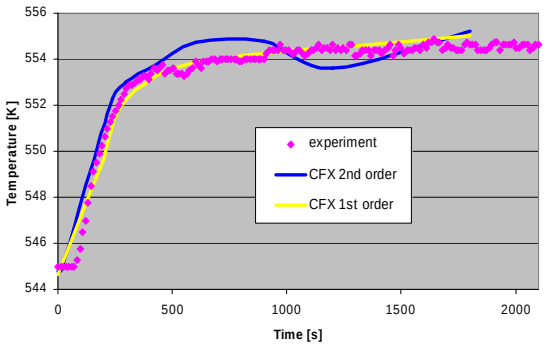


**Figure 10 Temperature at outlet of loop 1**

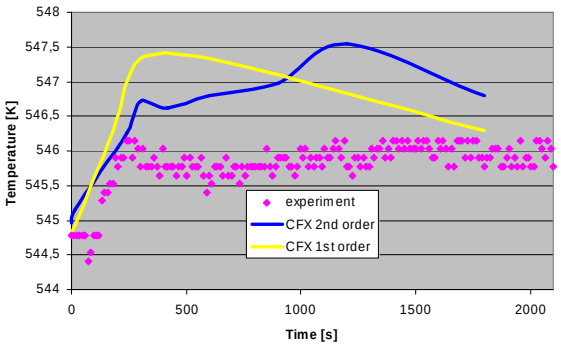


**Figure 11 Temperature at outlet of loop 2**

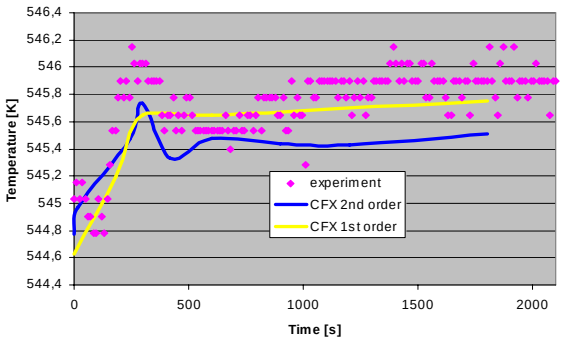


**Figure 12 Temperature at outlet of loop 3**

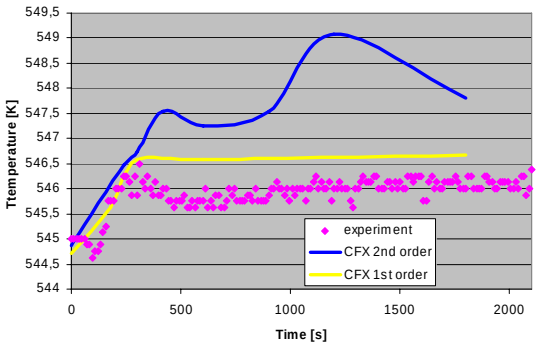


**Figure 13 Temperature at outlet of loop 4**

In loop 4 (Fig. 13) the temperature increase is clearly over-predicted by CFX-5 with the high-order method. It must be noted that the temperature rise of loops 2, 3 and 4 are much smaller than that of loop 1. The differences between plant data and numerical predictions are in all cases in the range of the measurement errors except for loop 4, especially between 1200 s and 1500 s where the numerical predictions of the 2nd order method are 3 K above the measurement data.

The CFX-5 results presented here reflect a dependency of the predictions on the discretization scheme and therefore on the spatial grid resolution. In the meantime the new code version CFX-10.0 provides a porous media model. The slotted parts of the support columns could now be simulated in a more realistic approach using this model. Furthermore it should be tried to resolve the perforations of the elliptic bottom plate by the grid. But these tasks would need both a new development of the grid for

this model part and some more computer memory. In general it can be mentioned that the most restrictive aspect during this work was the development of the computational grid especially for the upper plenum. The construction and testing of the respective model took around half a year.

## Conclusions and outlook

In this paper a detailed CFD model for a whole reactor pressure vessel of a PWR-reactor of VVER-1000 type including relevant in-vessel components for the post-test simulation of a coolant mixing test in the Kozloduy nuclear power plant, unit 6 is presented. The huge computer memory requirements of such a detailed model forced us to find a compromise between the degree of spatial resolution of some design details of the in-vessel components and the manageability of the model. Hence some elements in the lower plenum are modelled in a simplified way by additional pressure loss coefficients. The core is described in a simplified manner by 163 individual fuel assemblies while the upper plenum is fully resolved without simplifications. Nevertheless the final complete modular RPV-model consists of approximately 14 million cells.

Applying a 1$^{st}$ order donor cell method leads to a good agreement of calculated with plant data in case of a VVER1000 coolant mixing problem. For simulation of scenarios with significant feedback between the core neutronics and the thermal hydraulics a more frequently update of the core power is necessary for a more realistic description of the underlying physical phenomena by CFD-codes in such situations.

Further refinements of the presented model are still possible e.g. by using new features of CFX10.0 [8] e.g. the porous media model for the description of lower plenum components. However, success of the simulation demonstrated already, that CFD approaches are quite powerful to support the detailed physical understanding of complex experiments.

## References


1. F. Menter, et al.: CFD Best Practice Guidelines for CFD Code Validation for Reactor Safety Applications CFX Germany. February, 2002. Report EVOL-ECORA -D 01.
2. Kolev, N., Aniel,S., Royer, E., Bieder, U., Popov, D., Topalov, T. (2004). Volume 2: Specifications of the VVER-1000 Vessel Mixing Problems, Commissariat a l'Energie Atomique and OECD Nuclear Energy Agency, VVER-1000 Coolant Transient Benchmark (V1000CT).
3. Sánchez V., Böttcher, M.; Investigations of the VVER-1000 Coolant transient benchmark phase 1 with the coupled System Code RELAP5/PARCS. Paper sent to the Magazine Progress of Nuclear Energy for publication 2006.
4. Bieder, U. Bétin, S., Fauchet, G., Kolev, N. (2004). Preparation of the thermal hydraulic benchmark V1000CT-2.OECD/DOE/CEA. VVER-1000 Coolant Transient Benchmark, 2nd Workshop, Sofia Bulgaria.
5. Programs for the investigation of loop flow mixing in the reactor vessel of Kozloduy Unit 6 (1991). Kozloduy NPP.
6. Investigation of the loop flow mixing in the reactor vessel of Kalinin Unit 1 (1985). Kalinin NPP.
7. Barth, T.J., Jesperson, D.C. (1989). The Design and Application of Upwind Schemes on Unstructured Meshes. AIAA Paper 89-0366.
8. ANSYS CFX, Release 10.0 (2005). Reference Guide.